doi: 10.1111/j.1751-3928.2010.00112.x *Resource Geology* Vol. 60, No. 1: 18–34

Original Article

REE, Mn, Fe, Mg and C, O Isotopic Geochemistry of Calcites from Furong Tin Deposit, South China: Evidence for the Genesis of the Hydrothermal Ore-forming Fluids

Yan Shuang,[1,2] Xian-Wu Bi,[1] Rui-Zhong Hu,[1] Jian-Tang Peng,[1] Hang Li,[2] Da-Hua Li[2] and Chang-Sheng Zhu[2]

[1]*State Key Laboratory of Ore Deposit Geochemistry, Institute of Geochemistry, Chinese Academy of Sciences, Guiyang, China and* [2]*Chongqing Institute of Geology and Mineral Resources, Chongqing, China*

Abstract

The Furong tin deposit in the central Nanling region, South China, consists of three main types of mineralization ores, i.e. skarn-, altered granite- and greisen-type ores, hosted in Carboniferous and Permian strata and Mesozoic granitic intrusions. Calcite is the dominant gangue mineral intergrown with ore bodies in the orefield. We have carried out REE, Mn, Fe, and Mg geochemical and C, and O isotopic studies on calcites to constrain the source and evolution of the ore-forming fluids. The calcites from the Furong deposit exhibit middle negative Eu anomaly (Eu/Eu* = 0.311–0.921), except for one which has an Eu/Eu* of 1.10, with the total REE content of 5.49–133 ppm. The results show that the calcites are characterized by two types of REE distribution patterns: a LREE-enriched pattern and a flat REE pattern. The LREE-enriched pattern of calcites accompanying greisen-type ore and skarn-type ore are similar to those of Qitianling granite. The REE, Mn, Fe, and Mg abundances of calcites exhibit a decreasing tendency from granite rock mass to wall rock, i.e. these abundances of calcites associated with altered granite-type and greisen-type ores are higher than those associated with skarn-type ores. The calcites from primary ores in the Furong deposit show large variation in carbon and oxygen isotopic compositions. The $\delta^{13}C$ and $\delta^{18}O$ of calcites are –0.4 to –12.7‰ and 2.8 to 16.4‰, respectively, and mainly fall within the range between mantle or magmatic carbon and marine carbonate. The calcites from greisen and altered granite ores in the Furong deposit display a negative correlation in the diagram of $\delta^{13}C$ versus $\delta^{18}O$, probably owing to the CO_2-degassing of the ore-forming fluids. From the intrusion to wall-rock, the calcites display an increasing tendency with respect to $\delta^{13}C$ values. This implies that the carbon isotopic compositions of the ore-bearing fluids have progressively changed from domination by magmatic carbon to sedimentary carbonate carbon. In combination with other geological and geochemical data, we suggest that the ore-forming fluids represent magmatic origin. We believe that the fluids exsolved from fractionation of the granitic magma, accompanying magmatism of the Qitianling granite complex, were involved in the mineralization of the Furong tin polymetallic deposit.

Keywords: calcite, C, O isotopes, Furong tin deposit, ore-forming fluid, rare earth element.

Received 8 September 2008. Accepted for publication 3 March 2009.

Corresponding author: X.-W. BI, State Key Laboratory of Ore Deposit Geochemistry, Institute of Geochemistry, Chinese Academy of Sciences, Guiyang 550002, China., Email: bixianwu@vip.gyig.ac.cn

1. Introduction

In General, tin mineralization is genetically associated with highly differentiated S-type granite (Heinrich, 1990). A great number of studies on the genetic association of tin mineralization and S-type granites have been published in the last century (Taylor, 1979; Eugster, 1985; Schwartz & Askury, 1989; Heinrich, 1990; Lehmann & Harmanto, 1990; Pollard *et al.*, 1991). According to these documents, these granites are typical peraluminous and reduced, commonly enriched in W, Sn mineralized elements and volatiles such as F, Li and B. Generally, peraluminous magma is in favor of SnO_2 dissolution (Linnen *et al.*, 1996). At low oxygen fugacity, tin may be predominantly bivalent, and then favoring accumulation in the residual liquid and cause massive tin mineralization around the granites (Jackson & Helgeson, 1985; Linnen *et al.*, 1995, 1996). However, in recent years, there have been some tin deposits found to be genetically related to A-type granites (Sawkins, 1984; Nilson & Márcia, 1998). Usually, A-type granite magma is considered to be formed under relative low H_2O fugacity. In this case, it is difficult for the anhydrous magma to exsolve fluids (Loiselle & Wones, 1979; Collins *et al.*, 1982; Clemens, 1986). However, Bi (1999) disclosed that A-type granitoid rocks are not necessarily free from water and the water bearing A-type granites can also produce ore-forming fluids of geological interest through magmatic differentiation under certain conditions.

The Furong deposit is a newly-found giant tin polymetallic deposit in southern Hunan province, China. In a recent exploration, a 210,000-ton reserve of tin metal has been discovered (Chen & Liu, 2000; Huang *et al.*, 2001). Tin mineralized bodies mainly occur in the endo- and exo-contact zones of the southern part of the Qitianling granite intrusion, which has been shown to be of A-type (Zheng & Jia, 2001; Zhu *et al.*, 2005). A large number of detailed geologic, chronologic and petrologic studies have been published in recent years (Huang, 1992; Xu *et al.*, 2000; Huang *et al.*, 2001, 2003; Zheng & Jia, 2001, Cai *et al.*, 2002; Wei *et al.*, 2002; Wang *et al.*, 2003; Zhu *et al.*, 2003, 2005; Mao *et al.*, 2004; Peng *et al.*, 2007). These documents indicate an intimate temporal and special relationship between the tin mineralization and the Qitianling granite. There exist some discrepancies about the origin of the ore-forming fluid of the Furong deposit due to the lack of direct evidence from the deposit indicating the source of the ore-forming fluids. Wang *et al.* (2004) pointed out that the fluid/rock interaction of the exsolved fluid from the Qitianling pluton with the crystallizing granites has led to the widespread alteration and tin mineralization. Nevertheless, as deduced from mineralogy and H and O isotopic proof (Zhao *et al.*, 2005; Jiang *et al.*, 2006), the ore-forming fluid of the Furong deposit is influenced dominantly by meteoric water. This study attempts to establish an understanding of the source and the evolution of the ore-forming fluid, in the light of the REE geochemistry and carbon and oxygen isotopic data of the vein calcites associated with tin in the Furong deposit.

2. Regional and local geology

The Furong tin polymetallic deposit is located in the central part of the Nanling W-Sn mineralization district in Hunan province, China. The Nanling district lies in the north-western part of the Cathaysian block of South China (Fig. 1), which is mainly composed of Proterozoic basement overlain by a cover sequence of Sinian to Triassic sedimentary strata (Chen & Jahn, 1998). Regional NE-trending fault structures are well developed in the central Nanling district. Along these faults there intruded a great deal of granitoids, and numerous granite-related tin and tungsten deposits occur, including Shizhuyuan (Lu *et al.*, 2003), Yaogangxian (Peng *et al.*, 2006), Xianghualing (Yuan *et al.*, 2007), and Furong (Li *et al.*, 2006) (Fig. 1).

The Furong Sn-W deposit was discovered in the late 1990s and has a general ore grade of about 0.3–1.5% SnO_2 (Huang *et al.*, 2001). The proven reserve of tin ores is estimated to be about 600,000 tons (Wei *et al.*, 2002). The stratigraphic sequence mainly consists of Carboniferous carbonate rocks with silty and calcareous shale, and Permian carbonate rocks with ferromanganese chert, siliceous and calcareous shale, unconformably overlain by Cretaceous molasse (Fig. 2). A composite granitic stock, with an area of 520 km^2 intruded Carboniferous and Permian strata during Yanshanian. Three main intrusive phases were classified according to their petrology and intrusion ages: (i) medium- to coarse-grained porphyritic hornblende-biotite monzogranite with a zircon U-Pb age of 158.6–162.9 $\pm$ 0.4 Ma. The accessory minerals are apatite, sphene, zircon, magnetite and REE minerals; (ii) medium-grained porphyritic biotite granite with minor hornblende, has a zircon U-Pb age of 156.7–153.5 $\pm$ 0.4 Ma. The accessory minerals mainly consist of magnetite, ilmenite, zircon and REE minerals; (iii) some small fine-grained granites with an age of 147–143 Ma scatter

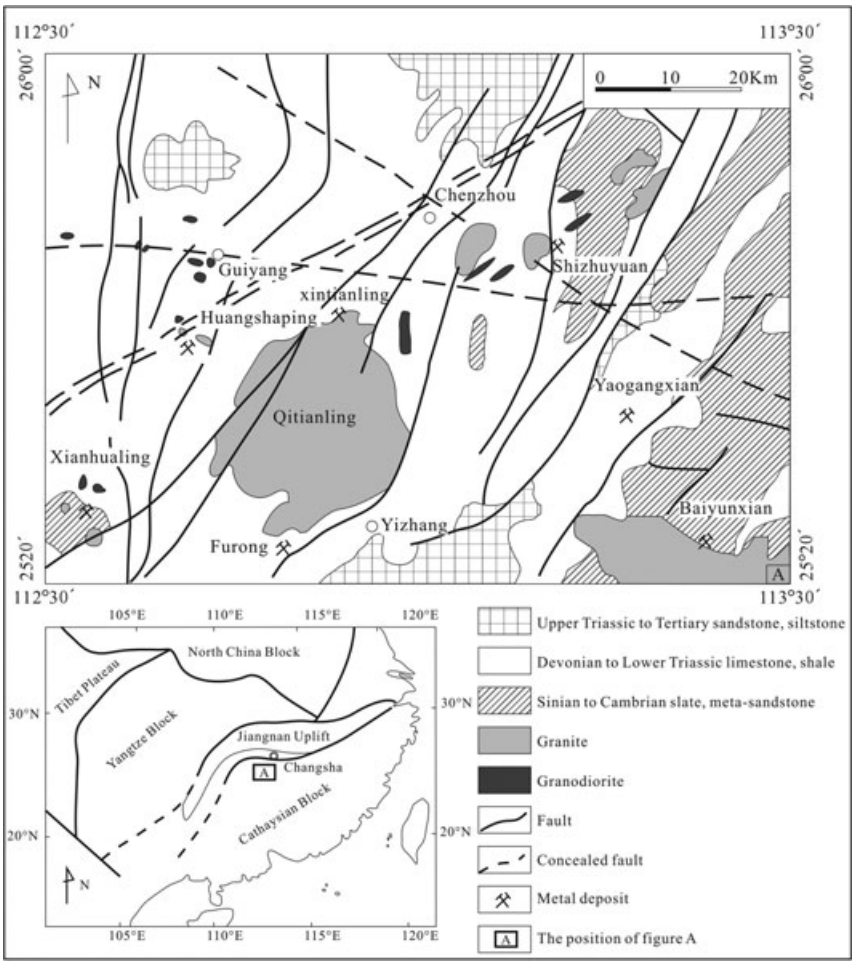

Fig. 1 Sketch map of tin deposits in central Nanling region, South China. Modified after Peng *et al.* (2006).

in the two granite phases mentioned above (Zhu *et al.*, 2005). The published data indicate that the intrusion stocks are enriched in Si, alkali and K, and might be assigned to A-type granite (Zheng & Jia, 2001; Zhu *et al.*, 2005). The Sn-W mineralization orebodies mainly occur along the endo- and exo-contact zones of the biotite granite (Fig. 2) and recent ^{40}Ar-^{39}Ar studies on mica reveal that tin mineralization in the Furong deposit took place at 150–160 Ma, quite similar to the intrusion age of the biotite granite (Peng *et al.*, 2007).

The Furong deposit consists of more than 50 ore veins. These veins are usually NE-striking, constituting three NE-trending tin ore blocks, i.e. Bailashui-Anyuan ore block, Heishanli-Maziping ore block, and Shanmenkou-Goutouling ore block (Fig. 2). There are three main types of primary tin mineralization identified in this deposit according to their mineralizing processes, hydrothermal alteration, and ore-hosted wall rocks, i.e. skarn-, altered granite- and greisen-type (Fig. 3).

In the Furong mining district, important tin-bearing skarns occur along the contact zones between the large composite Yanshanian granitic pluton and sedimentary strata in the Bailashui-Anyuan ore block. The productive Sn skarns have formed mainly at the zone of the exocontact, which mainly consists of diopside-hedenbergite, grossular-andradite, vesuvianite and wollastonite, with minor malayaite and cassiterite (Fig. 3a). They are characterized by strong deuteric alteration, especially amphibolization, chloritization, and phlogopitization. Sn mineralization is invariably related to these hydrothermal alterations (Fig. 3b). Cassiterite normally occurs as fine-grained dissemination (from <10 to about 500 μm) accompanied by hornblende, chlorite, phlogopite, quartz, calcite, magnetite with minor pyrite, chalcopyrite, bismuthinite, galena, sphalerite and arsenopyrite.

The altered granite is especially characterized by strong pervasive endogranitic chloritization (Fig. 3c). It has mainly been derived from porphyritic biotite

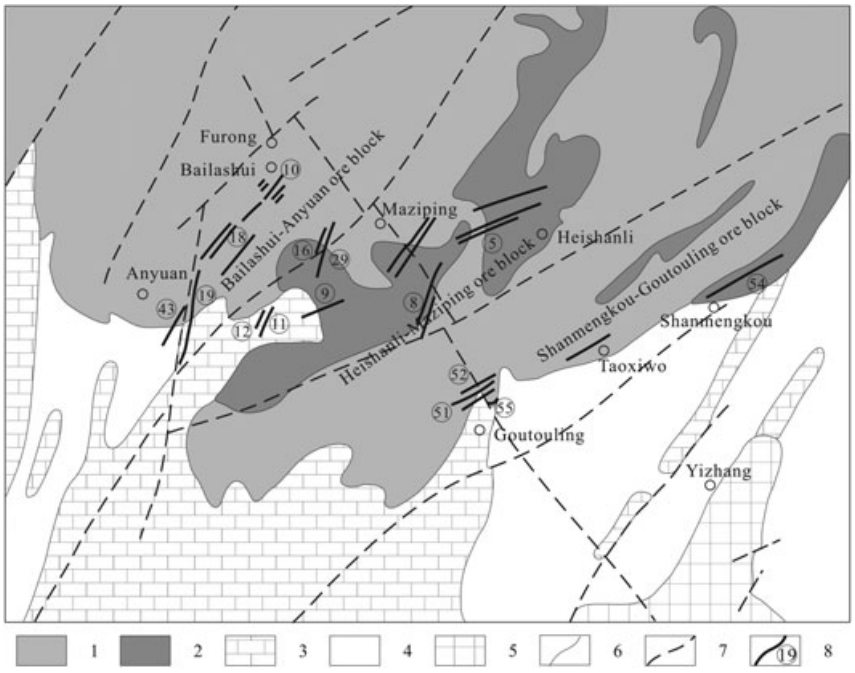

Fig. 2 Geological map of the Furong tin deposit, South China. Modified after Huang *et al.* (2003). 1: medium- to coarse-grained porphyritic hornblende-biotite monzogranite and biotite granite; 2: fine-grained granites; 3: Permian; 4: Carboniferous; 5: Cretaceous; 6: line of geological boundary; 7: faults; 8: ore-body and its serial number.

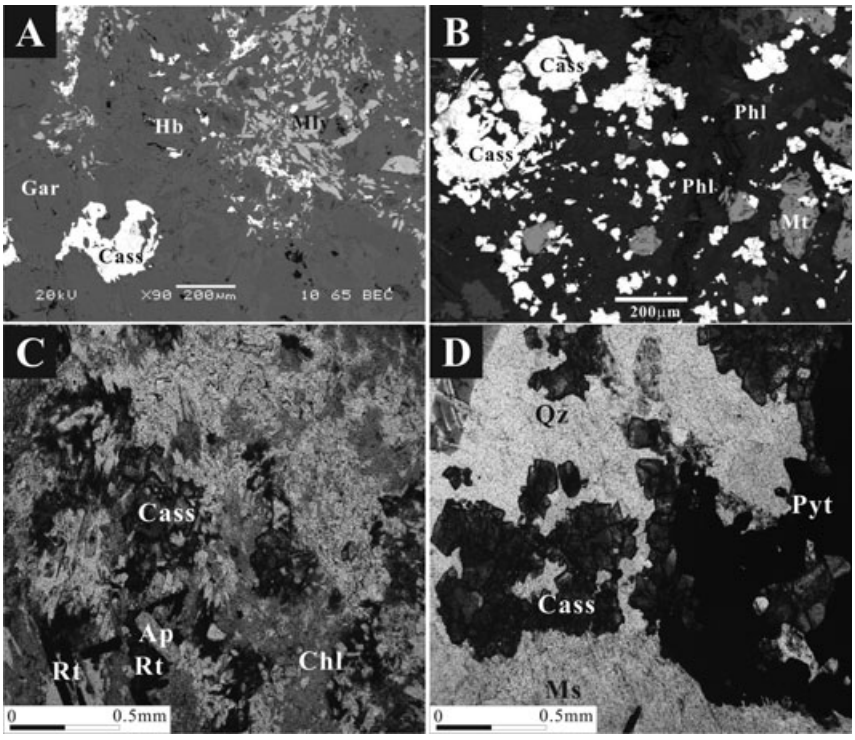

Fig. 3 Photographs of ores from the Furong tin deposit, South China. A: BSE image of skarn-type ore: cassiterite-garnet-hornblende-malayaite ore. B: BSE image of skarn-type ore: cassiterite-phlogopite-magnetite ore. C: Microscope image of altered granite-type ore: cassiterite-chlorite-rutile-muscovite-apatite ore. D: Microscope image of greisen-type ore: cassiterite-muscovite-quartz-pyrite ore. Abbreviations: Cass-cassiterite; Gar-garnet; Hb-hornblende; Mly-malayaite; Phl-phlogopite; Mt-magnetite; Rt-rutile; Ap-apatite. Chl-chlorite; Ms-muscovite; Qz-quartz; Pyt-pyrite.

granite. The transitional phase is the albitized and sericitized porphyritic biotite granite. Albite and sericite are characteristic products of deuteric alteration within the biotite granites forming at the expense of K-feldspar and biotite. Pervasive chlorite formed as veins and envelopes as a product of further fluid-rock interaction. Most of the cassiterites typically co-precipitated with rutile within the chloritized

granites. Cassiterite and rutile normally occur as fine-grained disseminations (50–1000 μm) together with chlorite, sericite, quartz and calcite. The ore minerals mainly consist of cassiterite with minor pyrite, chalcopyrite, galena and sphalerite.

The greisen mainly occurs within the porphyritic biotite granite along the south contact zone of the pluton and the strata. Tin mineralization is mainly associated with phyllic alteration occurring as disseminations in the greisenized granites and locally as quartz-sulfide veins (Fig. 3d). The mineral composition of the greisen varies from 30 to 80 percent quartz, 5–60 percent muscovite, and 0.5–10 percent sulfides. The typical quartz-rich greisen (>50 percent quartz) contains minor pyrite and arsenopyrite. Most of the cassiterite ore occurs within the greisen and the quartz bodies enclosed in it. The ore minerals, in order of decreasing abundance, are pyrite, arsenopyrite, chalcopyrite, cassiterite, rutile, sphalerite, galena, wolframinte and sheelite.

3. Samples and analytical methods

The calcite samples used in this study were collected from four representative ore lodes, i.e. No.10 and No.19 ore lodes in the Bailashui ore block, and No.55 ore lode in the Goutouling ore block in the Furong deposit. The specimens of skarn (FR19-1, FR19-2, FR19-3, FR19-4, FR19-5, FR19-6, FR19-7 and FR19-8) were sampled from No.19 lode in the Bailashui ore block, with calcites occurring as flesh-red nodules or veinlets intergrown with cassiterite, arsenopyrite, pyrite, chalcopyrite, galena and sphalerite (Fig. 4a); Samples FR55-3 and FR10-2 to FR10-4 were picked from No.55 lode in the Goutouling ore block and No.10 lode in the Bailashui ore block, with calcites of altered granite ore occurring as milk white veins which are often accompanied by fine-grained pyrite (Fig. 4b); Samples FR55-1, FR55-2, FR55-4 and FR10-1 were taken from greisen-type ores from No.55 lode in the Goutouling ore block and No.10 lode in the Bailashui ore block, with calcites occurring as fine-grained flesh-red or white nodules or plates associated with disseminated galena and pyrite (Fig. 4c). In order to constrain the association of the ore-forming fluids to the granites and wallrocks, we carried out REE and C, O isotopic studies on the Qitianling granite complex and limestone of the Qixia Group. The four hornblende-biotite monzogranite samples (FR-1, FR-2, FR-3 and FR-4) were from Qiguling in the Bailashui ore block and two of them (FR-3, FR-4)

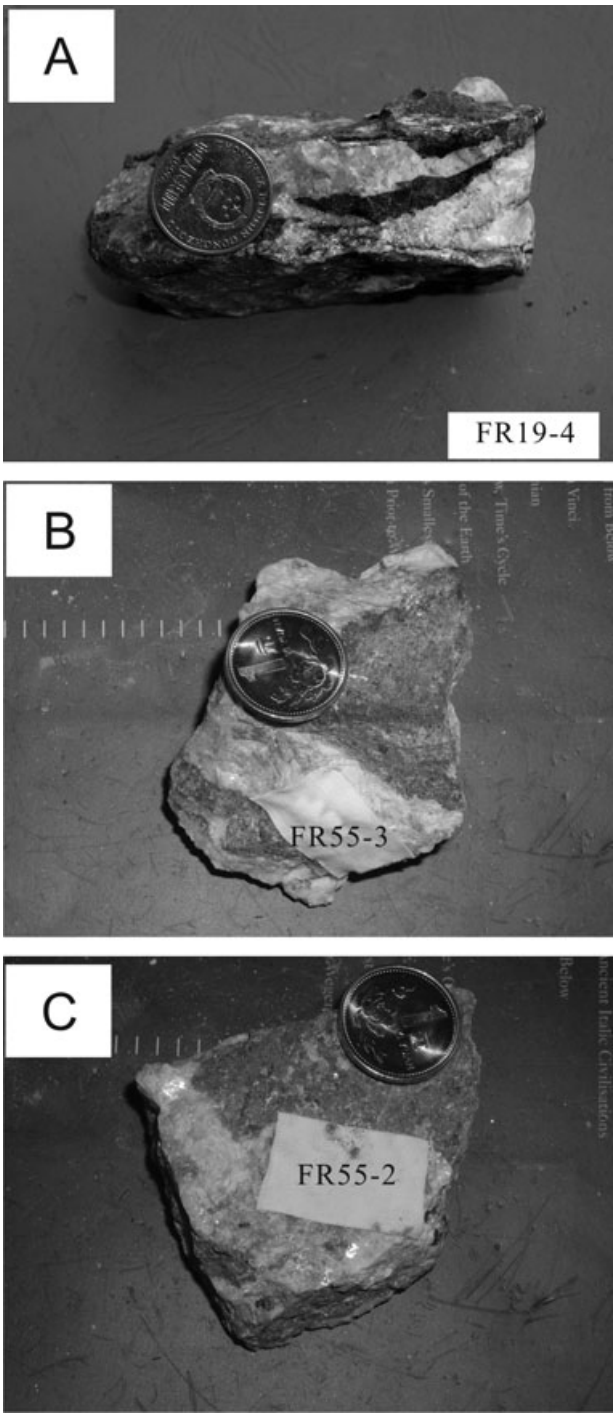

Fig. 4 Photographs of calcites from the Furong tin deposit, South China. (A)calcite associated with skarn type ore. (B) calcite associated with altered granite type ore. (C) calcite associated with greisen type ore.

are slightly chloritized. The remanent biotite granite samples were taken from the Goutouling ore block (FR-5 to FR-8), with two of them (FR-7, FR-8) slightly chloritized and muscovitized.

Rare earth elements of calcites and granites were determined by Inductively Coupled Plasma Mass Spectrometry (ICP-MS) at the laboratory of ICP-MS of Earth Department in Hong Kong University (Hong Kong), following the method proposed by Qi *et al.* (2000) with analytical error smaller than 5%. The Mg, Fe, and Mn compositions of calcites were analyzed by means of XRF in State Key Laboratory of Ore Deposit Geochemistry, Institute of Geochemistry, Chinese Academy of Sciences. The analytical error is smaller than 3%. Since the Ca content of calcite is 5–6 orders of magnitude higher than that of REE, theoretical Ca content was assumed in calculating the Yb/Ca ratio of calcite (Subías & Fernandez-Nieto, 1995).

The carbon and oxygen isotopic compositions were analyzed using the MAT 251 EM mass spectrometer (Institute of Mineral Resources, Chinese Academy of Geological Sciences, Bejing, China) at the Institute of Mineral Resources, Chinese Academy of Geological Sciences. In principle, samples were placed in the analyzer infused with 4 mL 100% phosphorate and then vacuumized for 2 h for keeping the pressure at 1.0 Pa. After full mixing of the phosphorate and the sample, place the analyzer into water with constant temperature of 25 ± 1°C for 5–6 h. CO_2 was separated by liquid nitrogen, and the purified CO_2 gas was introduced to mass spectrometer for the measurement of isotopic ratios. The analytical precision is ±0.2‰. The oxygen fractionation between calcite and water is calculated by means of O'Neil *et al.* (1969), using the average homogenization temperatures of fluid inclusions.

4. Results

4.1 The REE and Mn, Fe, Mg measurements

Table 1 lists the REE data and some characteristic parameters of calcites and also that of fresh and altered granites for companion. Figures 5 and 6 show the REE distribution patterns which were normalized using the chondritic composition of Boynton (1984). The Mg, Fe, and Mn analyzed data and the characteristic ratios of calcites are presented in Table 2.

As shown in Table 1 and Figure 5, in the Furong deposit, REE distribution patterns for calcites of greisen ores exhibit light rare earth elements (LREE) enriched (ΣLREE/ΣHREE = 3.05–6.24) and middle negative Eu anomaly (Eu/Eu* = 0.311–0.521) with the total REE content of 92.5–95.9 ppm. The calcites of altered granite ores have total REE contents varying from 27.2 to 133 ppm, with flat REE patterns (ΣLREE/ΣHREE ratios of 1.03–1.68) $(La/Yb)_N$ ratios of 0.687–0.908, and middle negative Eu anomalies (Eu/Eu* = 0.429–0.658). In contrast, the calcites of skarn-type ores display relatively low total REE abundances (ΣREE = 5.49–14.6 ppm) and LREE enrichment with ΣLREE/ΣHREE ratios of 2.58–6.91 and $(La/Yb)_N$ ratios of 2.47–9.42, and show moderate to light negative Eu anomalies (Eu/Eu* = 0.655–0.921), except for one with Eu/Eu* of 1.10.

As seen in Figure 6, the hornblende-biotite monzogranites from Bailashui area have similar REE features with light REE enrichment ($(La/Yb)_N$ ratios of 9.22–16.6), moderate negative Eu anomalies (Eu/Eu* = 0.439–0.535) and total REE abundance of 286 ppm to 516 ppm. The biotite monzogranites from the Goutouling area have lower REE abundances (ΣREE = 177 ppm~262 ppm) compared to those in the Bailashui area, and exhibit light REE enrichment patterns ($(La/Yb)_N$ = 3.53–6.39) and larger negative Eu anomalies (Eu/Eu* = 0.082–0.151). The differences between the hornblende-biotite monzogranite and the biotite monzogranite are shown in Figure 6a, b. The REE patterns of altered granites in both areas have similar features to each other, but compared to the fresh granites, have higher LREE levels (Fig. 6c, d).

As is clearly shown by Table 2, there is a decreasing tendency for Mn, Fe, and Mg contents of calcites from granite rock mass to wall rock, i.e. these contents of calcites associated with altered granite-type and greisen-type ores are higher than those associated with skarn-type ores. And relatively flat REE distributed calcites from altered ores have highest Mn abundances, then next to LREE-enriched calcites from greisen type ore-body and those from skarn-type ores have lowest.

4.2 C and O isotopic measurements

As listed in Table 3 and Figure 7, the calcites from primary ores in the Furong deposit show a large variation in carbon and oxygen isotopic compositions. Their $\delta^{13}C$ and $\delta^{18}O$ values are –12.7 to –0.4‰ and 2.8 to 16.4‰, respectively, contrasting with the spread in $\delta^{13}C$ and $\delta^{18}O$ values of calcites from other hydrothermal tin deposits in South China (Mao *et al.*, 2003). The carbon isotopic compositions of calcites in skarn are relatively stable, and have $\delta^{13}C$ of –3.3 to –0.4‰, with $\delta^{18}O$ of 2.8–7.8‰, yielding the $\delta^{18}O_{H2O}$ values of

Table 1 The REE compositions of calcites and granites from Furong tin deposit (ppm)

Sample	FR55-1	FR55-2	FR10-1	FR55-3	FR10-2	FR10-3	FR19-1	FR19-2	FR19-3	FR19-4	FR19-5	FR19-6	FR-1	FR-2	FR-3	FR-4	FR-5	FR-6	FR-7	FR-8
	Greisen-type ore			Altered granite-type ore			Skarn-type ore						Hornblende-biotite monzogranite		Chloritized hornblende-biotite monzogranite		Biotite granite		chloritized biotite granite	
La	15.5	16.2	15.5	3.94	12.9	3.08	3.47	2.31	3.07	1.95	2.13	1.63	73.7	59.1	105	117	33.4	41.6	46.8	56.5
Ce	33.1	33.8	37.6	7.70	30.0	7.30	5.68	3.62	4.74	3.48	2.54	2.01	141	122	251	271	69.7	91.1	92.4	113
Pr	3.86	3.96	4.82	0.963	3.69	0.971	0.667	0.600	0.541	0.426	0.377	0.240	15.6	14.1	21.5	20.5	8.27	11.2	10.6	12.4
Nd	13.7	14.0	19.2	4.07	15.4	3.63	2.17	2.28	1.88	1.21	1.20	0.535	54.2	50.4	72.9	63.2	28.4	39.7	34.7	40.3
Sm	4.10	4.09	4.83	1.74	7.36	1.73	0.578	0.843	0.372	0.366	0.356	0.199	10.2	9.96	12.8	10.2	6.83	10.2	7.30	8.17
Eu	0.409	0.477	0.760	0.303	1.81	0.356	0.122	0.200	0.091	0.127	0.088	0.065	1.42	1.62	1.84	1.47	0.177	0.252	0.283	0.380
Gd	3.93	3.88	4.11	2.69	9.58	1.84	0.564	0.911	0.393	0.343	0.368	0.233	8.41	8.63	9.71	10.3	6.12	8.59	6.53	7.27
Tb	0.807	0.762	0.634	0.672	2.61	0.437	0.088	0.171	0.061	0.054	0.059	0.037	1.32	1.39	1.36	1.57	1.23	1.58	1.20	1.27
Dy	5.56	5.30	3.82	5.40	19.1	2.77	0.492	1.070	0.383	0.327	0.360	0.211	7.05	7.73	7.12	8.47	7.64	9.74	7.28	7.82
Ho	1.20	1.08	0.734	1.19	3.76	0.534	0.097	0.219	0.081	0.069	0.078	0.046	1.43	1.54	1.44	1.63	1.70	2.05	1.57	1.70
Er	4.08	3.49	1.98	3.63	10.7	1.66	0.291	0.615	0.259	0.197	0.237	0.119	4.27	4.45	4.40	4.66	5.51	6.59	5.09	5.52
Tm	0.725	0.579	0.253	0.556	1.68	0.278	0.042	0.094	0.037	0.031	0.037	0.019	0.614	0.635	0.654	0.689	0.915	1.08	0.830	0.856
Yb	5.97	4.23	1.52	3.59	12.7	2.28	0.314	0.629	0.283	0.214	0.308	0.117	3.98	4.32	4.27	4.84	6.38	7.55	5.82	5.96
Lu	0.960	0.657	0.206	0.519	1.93	0.335	0.067	0.116	0.051	0.030	0.066	0.020	0.588	0.642	0.640	0.734	0.985	1.16	0.906	0.898
Y	40.7	39.6	28.0	75.6	121	18.8	4.07	10.2	4.62	2.68	2.94	2.03	40.2	40.0	40.72	45.6	49.4	63.1	48.4	51.3
ΣREE	94.0	92.5	95.9	37.0	133	27.2	14.6	13.7	12.2	8.82	8.19	5.49	323	286	495	516	177	232	221	262
LREE/HREE	3.05	3.63	6.24	1.03	1.15	1.68	6.48	2.58	6.91	5.97	4.42	5.84	10.7	8.76	15.74	14.7	4.81	5.06	6.57	7.38
Eu/Eu*	0.311	0.366	0.521	0.429	0.658	0.611	0.655	0.698	0.732	1.10	0.743	0.921	0.469	0.535	0.504	0.439	0.084	0.082	0.125	0.151
Ce/Ce*	1.03	1.02	1.05	0.951	1.05	1.02	0.898	0.742	0.886	0.919	0.682	0.774	0.997	1.01	1.27	1.34	1.01	1.02	1.00	1.03
$(La/Yb)_N$	1.76	2.58	6.88	0.741	0.687	0.908	7.45	2.47	7.32	6.14	4.65	9.42	12.5	9.22	16.6	16.2	3.53	3.71	5.42	6.39
$(La/Nd)_N$	2.19	2.24	1.56	1.87	1.62	1.64	3.10	1.96	3.15	3.12	3.44	5.91	2.63	2.27	2.79	3.57	2.27	2.03	2.61	2.72
$(La/Sm)_N$	2.38	2.49	2.01	1.43	1.11	1.12	3.78	1.72	5.19	3.35	3.76	5.17	4.55	3.73	5.16	7.18	3.07	2.56	4.03	4.35
$(Gd/Yb)_N$	0.532	0.740	2.19	0.605	0.610	0.649	1.45	1.17	1.12	1.29	0.964	1.61	1.71	1.61	1.84	1.72	0.775	0.918	0.905	0.985

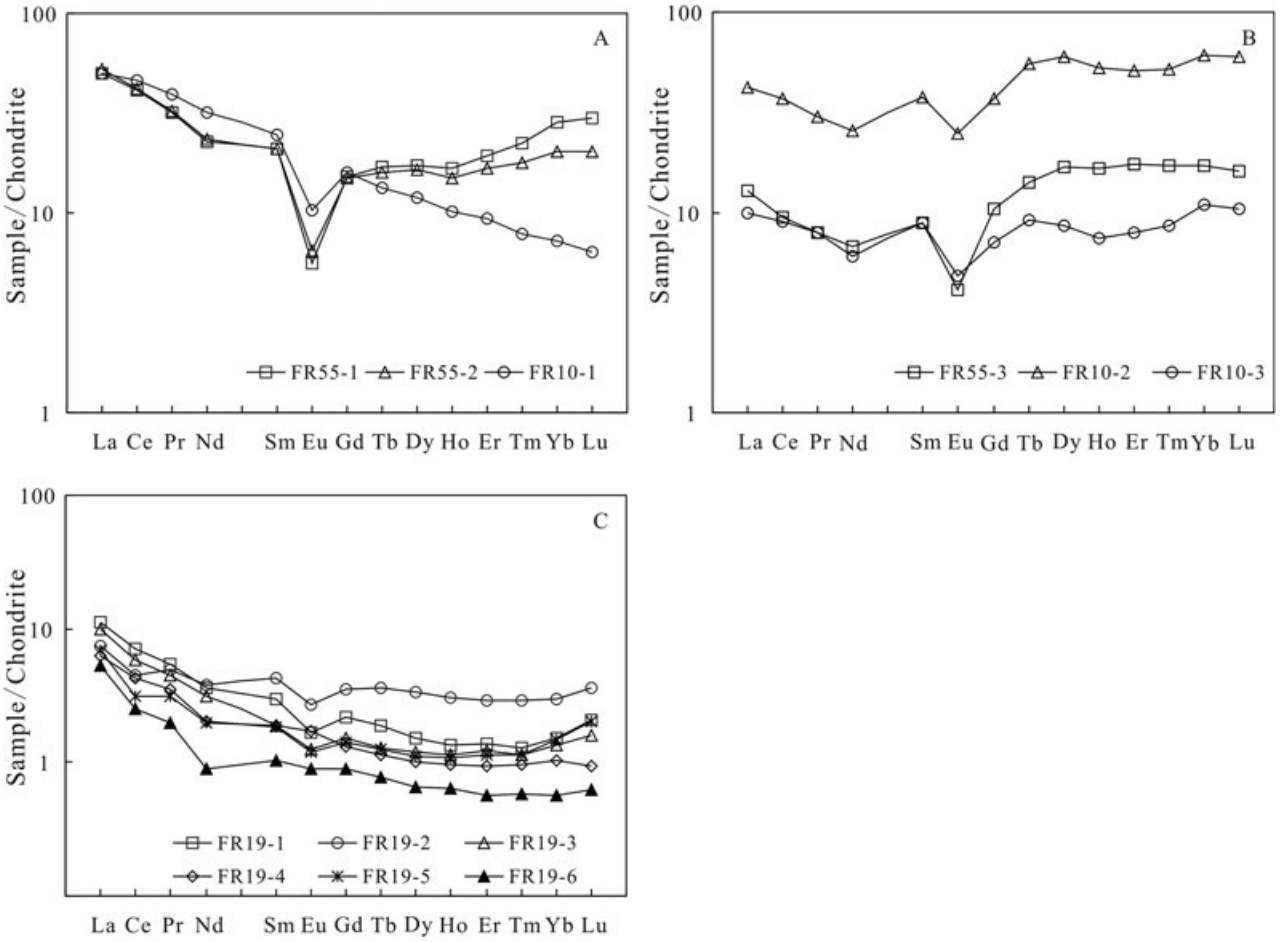

Fig. 5 Chondrite-normalized REE plot of calcites from Furong tin deposit. (a) Chondrite-normalized REE pattern of calcites from greisen-type ores; (b) Chondrite-normalized REE pattern of calcites from altered granite-type ores; (c) Chondrite-normalized REE pattern of calcites from skarn-type ores

0.4–5.4‰ for the hydrothermal water in equilibrium with calcites. In contrast, carbon and oxygen isotopic compositions of the calcites from greisen- and altered granite-type ores fall into quite a wide range. The $\delta^{13}C$ and $\delta^{18}O$ of calcites in greisen are –11.7 to –0.7‰ and 3.2 to 16.4‰, respectively, with $\delta^{18}O_{H2O}$ of –1.1–12.1‰. The calcites associated with altered granite ores have $\delta^{13}C$ and $\delta^{18}O$ values of –12.7 to –2.1‰ and 7.9–15.0‰, respectively, with $\delta^{18}O_{H2O}$ of water in equilibrium with them varying from 3.1 to 10.2‰. In order to evaluate accurately the role of the wall-rock interaction during mineralization, we also analyzed the carbon and oxygen isotopic compositions of the carbonate rocks around the orefield and the results show significant ^{13}C-enrichment ($\delta^{13}C$ = 0.6–2.6‰) with the $\delta^{18}O$ values of 18.8–20.3‰.

5. Discussion

5.1 REE geochemistry evidence of the origin of calcites

Inasmuch as the Yb/Ca-Yb/La diagram is a powerful tracer in the study of environment of formation and evolution of calcites (Möller & Morteani, 1983; Subías & Fernandez-Nieto, 1995), the Yb/Ca and Yb/La ratios of calcites from different types of ores have been plotted in the variation diagram proposed by (Möller & Morteani, 1983) (Fig. 8). The sample sets display a hydrothermal origin.

Y and Ho become geochemically decoupled in the presence of complexing agents. Bau & Dulski, (1995) invoked that the gangue minerals of same origin distribute approximately horizontally when plotted on

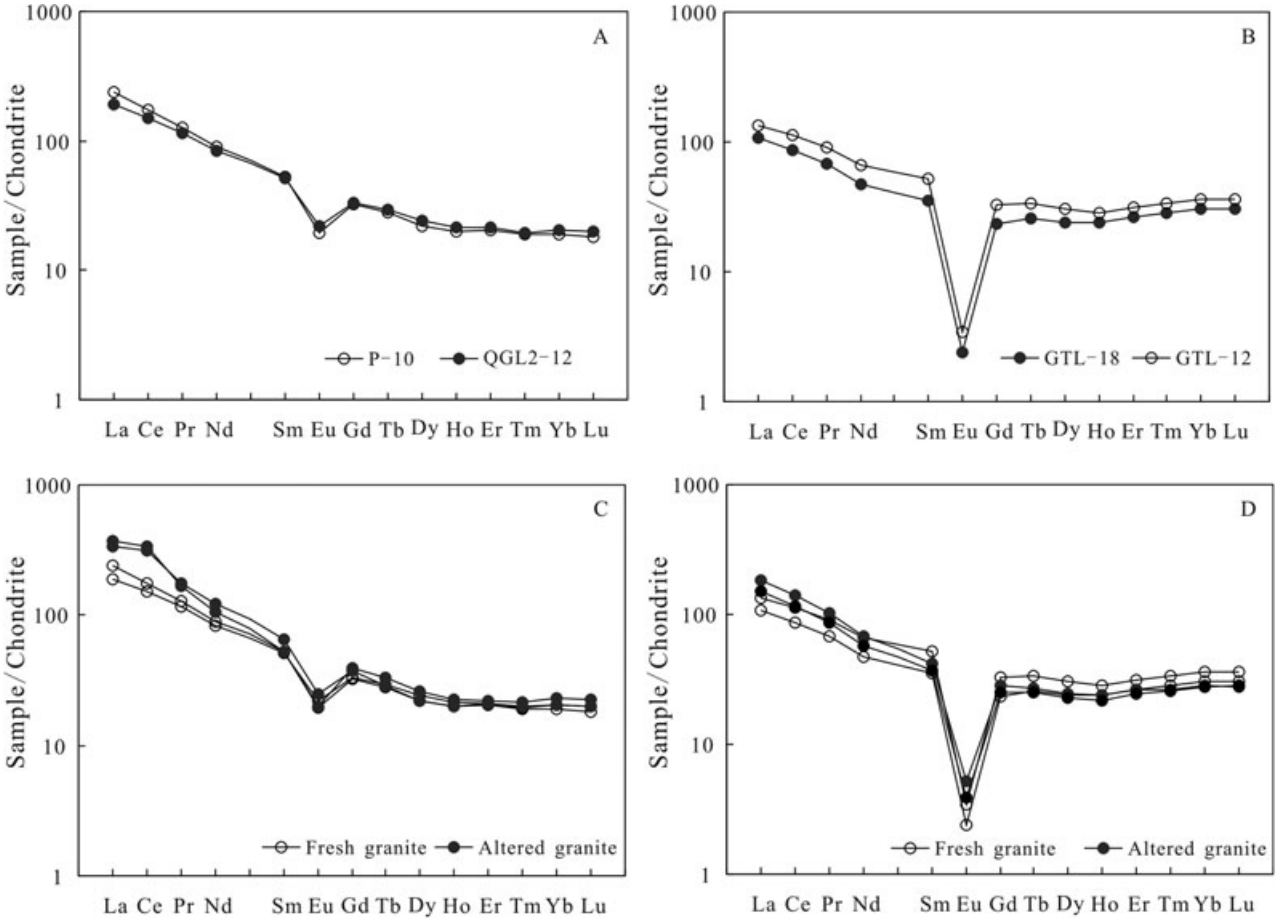

Fig. 6 Chondrite-normalized REE pattern of granites from Furong deposit. (a) REE distribution pattern of hornblende-biotite monzogranites. (b) REE distribution pattern of biotite granites. (c) contrast of the fresh monzogranites and chloritized monzogranites. (c) contrast of the fresh biotite granites and chloritized and muscovitized biotite granites.

Table 2 Mg, Fe, Mn compositions of calcites from the Furong tin deposit (wt%)

Sample	FR55-1	FR55-2	FR55-3	FR10-2	FR10-3	FR19-1	FR19-2	FR19-3	FR19-4	FR19-5
	Greisen-type ore		Altered granite-type ore			Skarn-type ore				
Mg	0.350	0.272	0.259	0.084	0.018	0.024	0.024	0.042	0.036	0.006
Fe	1.49	0.672	0.364	0.329	0.126	0.084	0.105	0.070	0.056	0.126
Mn	1.43	1.27	3.83	2.97	1.96	0.613	0.323	0.412	0.420	0.680
Mg+Fe+Mn	3.27	2.21	4.46	3.39	2.10	0.721	0.452	0.524	0.512	0.812
Mn/Mg	4.08	4.67	14.8	35.2	108	25.4	13.4	9.76	11.59	113
Mn/Fe	0.959	1.89	10.5	9.04	15.54	7.30	3.08	5.89	7.50	5.40

Y/Ho-La/Ho variogram, according to the research on geochemical evolution of the REE of fluorite and calcite from Tannenboden deposit and Beihilfe deposit in Germany. Although there is some discrimination in REE abundances, characteristics and distribution patterns between calcites from Bailashui-Anyuan and Shanmenkou-Goutouling ore blocks in the Furong deposit, these calcites may be of the same sources since they are mainly distributed horizontally in the Y/Ho-La/Ho variogram (Fig. 9).

Table 3 Carbon and oxygen isotopic compositions of calcites and wallrocks from Furong deposit (‰)

Sample	Mineralized type	Minerals	$\delta^{13}C$ (‰)	$\delta^{18}O$ (‰)	$\delta^{18}O_{H2O}$ (‰)	Average homogenization temperature
FR19-1	Skarn-type ores	Calcite	–1.5	4.4	2.0	450
FR19-2		Calcite	–1.8	6.6	4.2	450
FR19-3		Calcite	–1.5	2.8	0.4	450
FR19-4		Calcite	–0.4	7.3	4.9	450
FR19-5		Calcite	–2.9	7.5	5.1	450
FR19-6		Calcite	–0.9	7.8	5.4	450
FR19-7		Calcite	–1.7	5.2	2.8	450
FR19-8		Calcite	–3.3	4.7	2.3	450
FR55-1	Greisen-type ores	Calcite	–0.7	3.3	–1.0	350
FR55-2		Calcite	–1.0	3.2	–1.1	350
FR55-4		Calcite	–6.1	9.8	5.5	350
FR10-1		Calcite	–11.7	16.4	12.1	350
FR10-2	Altered granite-type ores	Calcite	–2.1	9.0	4.2	330
FR10-3		Calcite	–2.4	9.6	4.8	330
FR10-4		Calcite	–12.7	15.0	10.2	330
FR55-3		Calcite	–3.4	7.9	3.1	330
LJD-1	Wall rocks	Limestone	0.6	18.8		
LJD-2		Limestone	1.8	19.4		
LJD-3		Limestone	2.6	20.3		

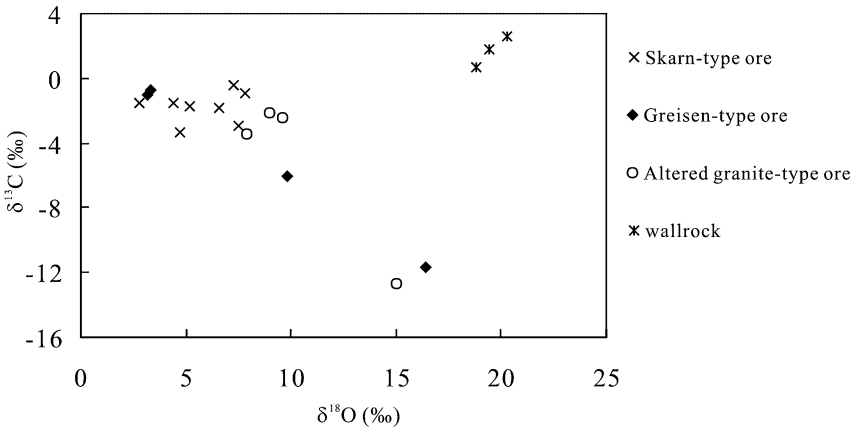

Fig. 7 The δ13C versus δ18O diagram for calcites from the Furong tin deposit, South China.

5.2 REE and Mn, Mg, Fe geochemistry of the source of the hydrothermal fluids

Rare earth element geochemistry indicates that the calcites were deposited from the hydrothermal fluids. The intimate spatial and temporal association between the Qitianling granite intrusion and tin mineralization in the Furong tin deposit emphasizes the genetic role of magmas in the mineralization process. Calcite is the dominant hydrothermal mineral distributed widely in different ore types in the Furong tin deposit. Therefore, there are two possible sources for the hydrothermal fluids which precipitated calcites: (1) External fluids drawn into a hydrothermal convection system by the heat of the magmatic intrusion, and (2) magmatic fluids concentrated by crystallization of the Qitianling granite rocks.

Rare earth element solubilities in hydrothermal fluids are extremely low, as observed on the East Pacific rise by Michard *et al.* (1983). Country rocks tend to retain most of their REE during hydrothermal alteration (Michard, 1989). Exploring alternative (1) above, low-temperature fluids entering a hydrothermal system from the country rocks would have contained low concentrations of REE, but could have taken them up from the granites as they were

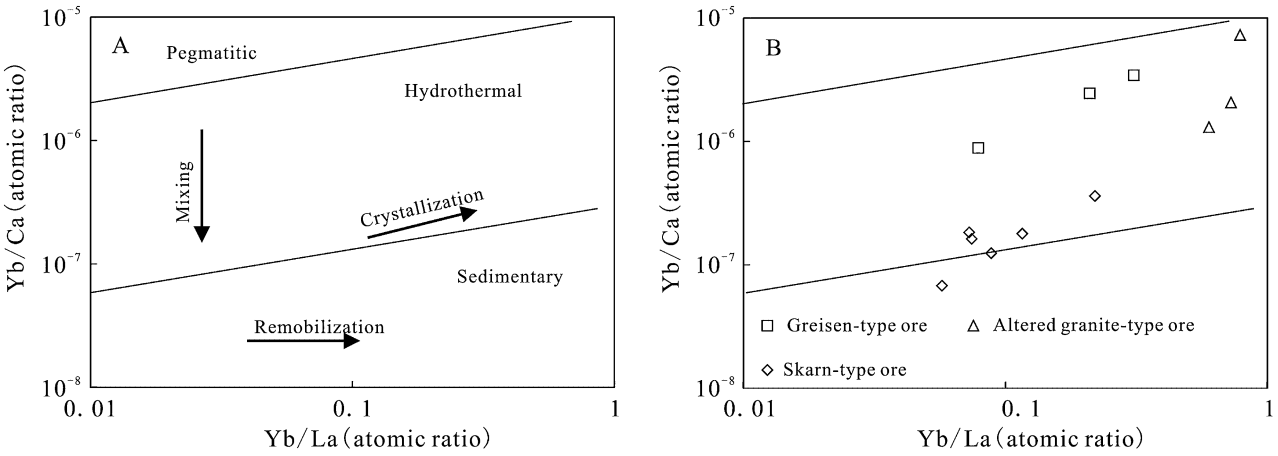

Fig. 8 Yb/Ca-Yb/La diagrams of calcites. (a) Schematic Yb/Ca-Yb/La diagram after Möller and Morteani (1983); (b) All the calcites from Furong deposit fall into hydrothermal field in Yb/Ca-Yb/La diagram.

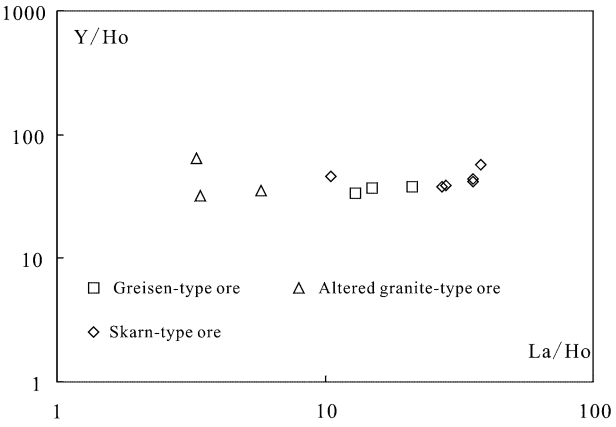

Fig. 9 Y/Ho-La/Ho diagram of calcites.

heated up. But REE contents of altered granites in both areas are higher than those of fresh granites, indicating that the hydrothermal fluid did not take REEs from the fresh granites. External fluids also seem unlikely to have contained the high concentrations of anions needed to form complexes with and dissolve the large amounts of REE which the fluids must have contained. The abundance of Mn in the calcites (0.323–3.83 wt %) is higher than that of the fresh granite (0.04–0.012 wt %).

Most magmas exsolve fluids during their ascent through the middle to upper crust and such magmatic-hydrothermal fluids are enriched metals and ligands (Hedenquist & Lowenstern, 1994). In their study of fluid inclusions from igneous rocks in New Mexico, USA, Banks *et al.* (1994) found that the post-magmatic stage of hydrothermal solutions could carry large amounts of REE up to 1300 ppm, due to such fluids containing abundant complex-forming anions. The solubility and the liquid-solid distribution coefficients of REE are greatly increased by complexing agents such as Cl, F, and CO_2 (Schade *et al.*, 1989). It is concluded that the post-magmatic hydrothermal fluid in the studied area is enriched in Mn based on research data presented before (Li, 1995a, b). The Mn content of calcites from greisen-type and altered granite-type ores range from 1.27 to 3.83 wt %, very close to the Mn contents of calcites of magmatic hydrothermal origin, which average from 1.88 to 2.65 wt % (Li, 1995b). Therefore, the higher Mn, Fe, and Mg abundances of calcites from greisen-type and altered granite-type ores and REE characteristics of magma exsolution fluids allow us to deduce that the hydrothermal fluid from which the calcites were deposited is magmatic, evolved by crystallization of the Qitianling granite rocks.

5.3 REE and Mn, Mg, and Fe geochemistry of the evolution of the hydrothermal fluids

In general, the REE patterns of hydrothermal minerals depend significantly on the crystal configuration and the stability of REE complexation in hydrothermal system (Mineyev, 1963; Morgan & Wandless, 1980; Michard, 1989). However, in recent years more authors have concluded that the REE distribution is preferentially susceptible to the stability of REE complexation compared to crystallographic factors (Terakado & Masuda, 1988; Wood, 1990; Lottermoser, 1992; Haas

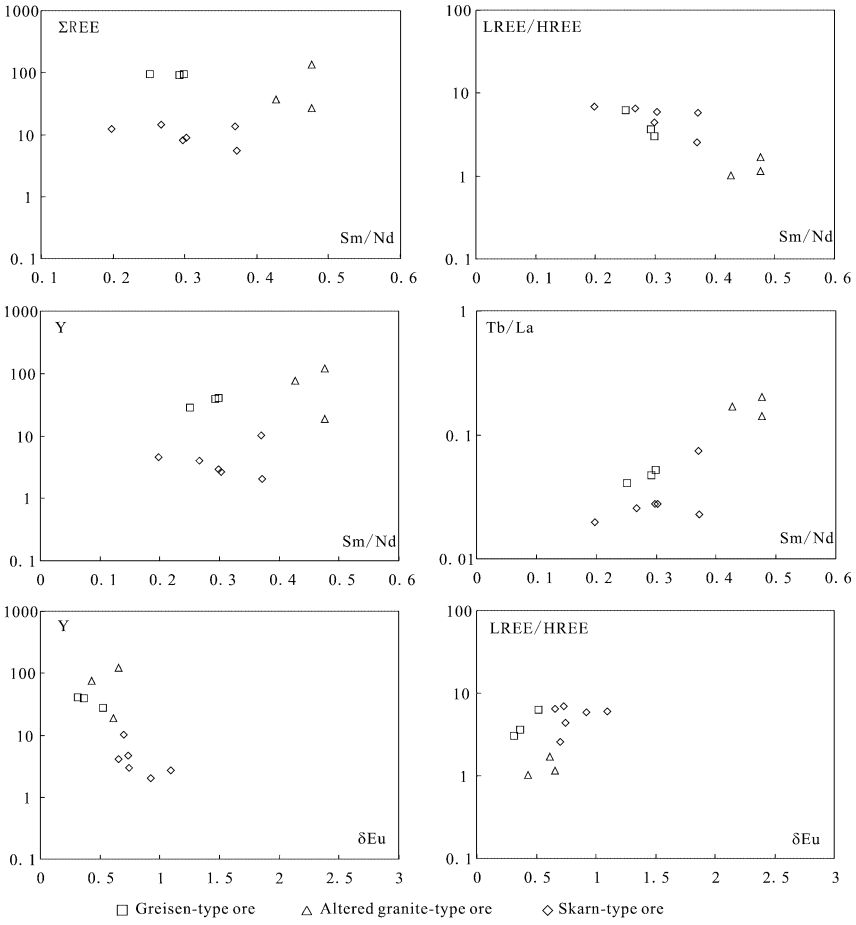

Fig. 10 Variation diagram of REE in calcites.

et al., 1995). It is indicated by previous studies that all REEs are characterized by REE complexations in solution, and that the REE complexations with CO_3^{2-} and HCO_3^- are predicted to become more stable while the REE atomic number increases (Dumonceau *et al.*, 1978; Cantrell & Byrne, 1987; Wood, 1990; Lee & Byrne, 1993; Haas *et al.*, 1995; Zhong & Mucci, 1995).

As mentioned above, those calcites deposited from magmatic fluids evolved by crystallization of the Qitianling granite rocks show the different REE patterns. The hydrothermal calcites from Bailashui and Goutouling ore blocks all have LREE-enriched patterns and flat REE patterns. The REE patterns of calcites occurring as nodules and veinlets in greisen-type and skarn-type ores display an LREE-enriched pattern, and those in altered granite ores, which appear as veins, have flat REE patterns. The REE variation diagrams for calcites show a continuous distribution trend of both the calcites of LREE-enriched and nearly flat REE (Fig. 10), suggesting that these homologous calcites are not precipitated contemporaneously.

Those calcites are formed in the post-stage during the mineralization period in the Furong tin deposit. It is observed from Figure 6c, d that the LREE abundances distinctly increased from fresh granite to altered granite, indicating obvious LREE leaching during alteration. Accordingly, the nearly flat REE patterns of calcites from altered granite ores represent the REE distribution patterns of the relic hydrothermal fluid achieved by LREE leaching. As shown in Figures 5 and 6, the LREE-enriched patterns of calcites from greisen-type and skarn-type ores are very similar to those of the fresh granites in both the Bailashui ore block and the Goutouling ore block. This close correspondence suggests that there is little LREE leaching during the mineralization period, and that the relic hydrothermal fluid has inherited REE geochemistry characteristics of magmatic fluids concentrated by crystallization of the Qitianling granite rocks. To conclude this, both LREE-enriched pattern and flat-REE pattern calcites were precipitated contemporaneously from the same hydrothermal fluid.

As is clearly shown in Tables 1 and 2, there is a decreasing tendency for REE, Mn, Fe, and Mg abundances of calcites from altered granite-type and greisen-type ores to skarn-type ores. The REE, Mn, Fe, and Mg abundances of calcites from skarn-type ores distributed along the contact zone between granite rocks and wall-rocks are relatively lower. This geological fact might indicate that the hydrothermal fluid precipitated skarn-type ores is much affected by the original rocks, and the earlier crystallization of Mn-, Fe- and Mg-bearing skarn minerals also bring out substantive Mn, Fe, Mg and REE from the system.

5.4 C, O isotopic geochemistry and its geological implication

Calcite C-O isotope geochemistry has been used elsewhere to trace the origin of hydrothermal fluids (Ohmoto & Rye, 1970; Rye *et al.*, 1974; Zheng, 1990; Zheng & Hoefs, 1993). The present results show that all $\delta^{13}C$ values of calcites from the Furong tin deposit fall within the range between mantle or magmatic carbon (–3 to –9‰) (Ohmoto, 1972; Rollinson, 1993), crustal carbon (Craig, 1953; Fuex & Baker, 1973) and marine carbonate. However, the $\delta^{18}O_{H2O}$ values of hydrothermal fluids in equilibrium with calcites mainly vary from 3.1 to 4.9‰, obviously higher than the $\delta^{18}O_{H2O}$ value of the meteoric water in southern China during the Mesozoic (–9‰) (Zhang, 1985). As a matter of fact, these $\delta^{18}O_{H2O}$ values are very close to the magmatic fluids (6–8‰) (Taylor, 1974). These characteristics imply that the hydrothermal fluids from which these calcites were deposited mainly have a magmatic origin.

As depicted in Figure 7, a negative correlation between $\delta^{13}C$ and $\delta^{18}O$ values is observed for calcites from greisen and altered granite ores in the Furong tin deposit. In general, three types of geological processes can be distinguished as responsible for the precipitation of calcites: (1) fluid/rock interaction (2) mixing of fluids, and (3) CO_2 degassing (Zheng, 1990; Zheng & Hoefs, 1993). The mixing of the fluids is characterized by simultaneous presence of more than two types of fluids of different carbon and oxygen compositions. Additionally, one of them has a $\delta^{13}C$ value lower than –12.7‰, much lower than mantle or magmatic carbon. In view of fluid of various sources, this does not explain the present isotopic features. A large number of documents have published evidence that the fluid/rock interaction might lead to a positive correlation between $\delta^{13}C$ and $\delta^{18}O$ values (Zheng, 1990; Zheng & Hoefs, 1993; Peng & Hu, 2001). Fluid/rock interaction is therefore not likely to have been significant in the process of calcite precipitation. The discovery of the coexistence of CO_2–rich inclusions and H_2O-rich inclusions and high salinity inclusions in greisen and altered granite ores and their similar homogeneous temperatures during our study of fluid inclusions of the Furong tin deposit suggest the existence of CO_2 degassing during mineralization. Theoretically, the degassing of CO_2 can cause distinct depletion in $\delta^{13}C$ (Zheng & Chen, 2000). If calcite is deposited from hydrothermal solutions when HCO_3^- act as the dominant dissolved carbon species due to CO_2 degassing, the resulting calcite has a negative $\delta^{13}C$-$\delta^{18}O$-correlation (Zheng, 1990; Morishita, 1993; Morishita & Nakano, 2008). Therefore, degassing of CO_2 is assumed as a process to cause precipitation of calcite in this mining area.

5.5 Other evidence of the origin of the ore-forming fluid

Zhao *et al.* (2005) argue that the Qitianling granitic magma has a high oxygen fugacity according to the mineralogical evidence and that tin is incorporated in mafic minerals during early stages of crystallization and not enriched in later residual liquid. Accordingly, they proposed the surface-derived origin for ore-forming solution during the tin mineralization, most probably involving meteoric water. In view of the geochemistry of the Qitianling granite, this argument does not stand under close scrutiny, because the mineralized lodes mainly occur along the south endo- and exo-contact zones of the biotite granite in the Qitianling granite complex and the wallrocks. The electron microprobe analysis results of biotite from biotite granite support a lower oxygen fugacity for the magma and higher F and lower Cl contents, in contrast to the results of hornblende-biotite monzogranite (Li *et al.*, 2007a). Theoretically, fluorine enters into the melt and $D_{Cl,\ fluid/melt}$ decreases logarithmically with increasing F content of the melt during magma crystallization (London, 1987; Webster & Holloway, 1990). Fluorine has no major influence on the $D_{Sn,fluid/melt}$. However, it increases substantively with increasing Cl-content of the hydrothermal fluid system (Taylor & Wall, 1984; Lehmann, 1990; Keppler & Wyllie, 1991; Halter *et al.*, 1998; Audétat *et al.*, 2000). A large number of published data document that at high oxygen fugacity, tin may be present in the tetravalent state and be incorporated into the mineral lattice of magnetite and hornblende during early stages of crystallization,

and that at low fO_2, tin may be predominantly bivalent, and then favoring accumulation in the residual liquid (Jackson & Helgeson, 1985; Linnen *et al.*, 1995, 1996). From the above, the magmatic hydrothermal fluids exsolved directly from biotite granite are expected to be enriched in Cl and Sn.

The newly published ^{40}Ar-^{39}Ar plateau ages of phlogopite, muscovite, and hydrothermal hornblende from Bailashui and Taoxiwo ore districts in Furong deposit fall into the range of 150–160 Ma (Peng *et al.*, 2007), consistent with earlier Ar isotope data by Mao *et al.*, (2004). All available dating evidence (Huang, 1992; Zhu *et al.*, 2003, 2005; Fu *et al.*, 2004; Mao *et al.*, 2004) points a mid-late Jurassic age (150–163 Ma) for the main part of the Qitianling pluton. These chronologic data and the distribution of mineralized lodes suggest close spatial and temporal relationships of mineralization to the granite emplacement. This implies that the Qitianling granite emplacement was essential for the mineralization process as well as the hydrothermal processes. As shown before, the REE and C-O isotopic geochemistry of calcites from the Furong deposit provides information on the magmatic hydrothermal origin for the tin mineralization, probably involving surface-derived meteoric water. This also agrees with the results from sulfur, lead and helium isotopic geochemistry (Li *et al.*, 2006; Li *et al.*, 2007b).

According to Wang *et al.* (2004), the following arguments are derived to support high-salinity magmatic-hydrothermal fluids enriched in CO_2 exsolved from the intrusion: (i) Qitianling granite is characterized by many unequilibrium textures and structures, such as porphyritic, seriate, graphic, granophyric, myrmekitic, and aplitic textures, and pegmatoid and miarolitic structures; (ii) Quartz in the granite contains melt inclusions which coexist with CO_2 inclusions and high-salinity inclusions; (iii) Qitianling granite, widely altered, especially with the occurence of high-temperature auto-metasomatism albitization and microclinization of perthite. During our ongoing fluid inclusions study, daughter mineral-bearing inclusions and CO_2-rich three phase inclusions have been observed in gangue minerals associated with ores. Li and Liu (2005) have presented microthermometric measurement of homogenization and salinity data of fluid inclusions of gangue minerals from skarn and granites. These inclusions homogenize at 290–560°C, have salinities of 47–67 wt % $NaCl_{equiv}$, and contain substantive CO_2. This implies that the ore-forming fluid in the deposit is characterized by high salinity and CO_2-enrichment. This is consistent with the hypothesis that hydrothermal fluids exsolved from Qitianling granite intrusion, and that the mineralizing fluids in the deposit were closely associated with the emplacement of the Qitianling granite.

6. Conclusions

Calcite occurs extensively in the Furong deposit, appearing as nodules, veinlets and veins in various type ores. The REE, Mn, Mg, and Fe contents and C, and O isotopic geochemical characteristics of these calcites, suggest that the magmatic-hydrothermal fluid concentrated by crystallization of the Qitianling granite intrusion was a significant source of the ore-forming hydrothermal fluid in the Furong tin deposit.

Acknowledgments

This research project was financially supported jointly by National Basic Research Program of China (2007CB411404), the National Natural Science Foundation of China (40673042,40373020), "CAS Hundred Talents" Project from Chinese Academy of Sciences to R. Z. Hu and the Chinese Academy of Sciences Innovational Program (KZCX3-SW-125). The authors thank the personnel of the geological Survey of South Hunan, Hunan Bureau of Geology and Mineral Resources for their earnest help during our fieldwork. We are also grateful to Professor M. F. Zhou and Dr L. Qi of the Earth Department in Hong Kong University and Dr C. X. Feng of the State Key Laboratory of Ore Deposit Geochemistry, Institute of Geochemistry, Chinese Academy of Sciences for providing facilities in chemical analysis. Drs Hidehiko Shimazaki and Yuichi Morishita are thanked for their careful and thoughtful comments and suggestions that helped to improve this paper. Guidance from the editors, Drs Yoshimichi Kajiwara and Yasushi Watanabe, is acknowledged with thanks.

References

Audétat, A., Günther, D. and Heinrich, C. A. (2000) Magmatic-hydrothermal evolution in a fractionating granite: a microchemical study of the Sn-W-F-mineralized mole granite (Australia). Geochim. Cosmochim. Acta, 64, 3373–3393.

Banks, D. A., Yardley, B. W. D., Campbell, A. R. and Jarvis, K. E. (1994) REE composition of an aqueous magmatic fluid: a fluid inclusion study from the Capitan Pluton, New Mexico, U.S.A. Chem. Geol., 113, 259–272.

Bau, M. and Dulski, P. (1995) Comparative-study of yttrium and rare-earth element behaviors in fluorine-rich hydrothermal fluids. Contrib. Mineral. Petrol., 119, 213–223.

Bi, X. W. (1999) Alkali-rich intrusive rocks in the "Sanjiang" (three-river) region, western Yunnan and their relation with metallogenesis of copper and gold. PhD Thesis, The institute of geochemistry, Chinese Academy of Sciences, Guiyang, 98p.

Boynton, W. V. (1984) Cosmochemistry of the rare earth elements: meteorite studies. In Henderson, P. (ed.) Rare earth element geochemistry. Elsevier, Amsterdam, 63–114.

Cai, J. H., Mao, X. D., Cai, M. H. and Liu, G. Q. (2002) Geological characteristics of Bailashui tin deposit in Qitianling orefield, Southern Hunan province. Geol. Mineral Resour. South China, 2, 54–59 (in Chinese with English abstract).

Cantrell, K. J. and Byrne, R. H. (1987) Rare earth element complexation by carbonate and oxalate ions. Geochim. Cosmochim. Acta, 51, 597–605.

Chen, J. F. and Jahn, B. (1998) Crustal evolution of southeastern China: Nd and Sr isotopic evidence. Tectonophysics, 284, 101–133.

Chen, M. S. and Liu, X. H. (2000) Metallogenic model and resource general capacity forecast of Furong Sn field in Chenzhou. Hunan Geol., 19, 43–47 (in Chinese with English abstract).

Clemens, J. D. (1986) Origin of an a-type granite: experimental constraints. Am. Mineral., 7, 317–324.

Collins, W., Beams, S., White, A. and Chappell, B. (1982) Nature and origin of A-type granites with particular reference to southeastern Australia. Contrib. Mineral. Petrol., 80, 189–200.

Craig, H. (1953) The geochemistry of the stable carbon isotopes. Geochim. Cosmochim. Acta, 3, 53–92.

Dumonceau, J., Bigot, S., Treuil, M., Faucherre, J. and Fromage, F. (1978) Détermination des constants de formation des tetracarbonatolanthanides(III). C. R. Acad. Sci. Paris Sér. C, 287, 325–327.

Eugster, H. P. (1985) Granites and hydrothermal ore deposits: a geochemical framework. Mineral. Mag., 49, 7–23.

Fu, J. M., Ma, C. Q., Xie, C. F., Zhang, Y. M. and Peng, S. B. (2004) Zircon SHRIMP dating of the Cailing granite on the eastern margin of the Qitianling granite, Hunan, South China, and its significance. Geol. China, 31, 96–100 (in Chinese with English abstract).

Fuex, A. N. and Baker, D. R. (1973) Stable carbon isotopes in selected granitic, mafic, and ultramafic igneous rocks. Geochim. Cosmochim. Acta, 37, 2509–2521.

Haas, J. R., Shock, E. L. and Sassani, D. C. (1995) Rare earth elements in hydrothermal systems: estimates of standard partial molal thermodynamic properties of aqueous complexes of the rare earth elements at high pressures and temperatures. Geochim. Cosmochim. Acta, 59, 4329–4350.

Halter, W. E., Williams-Jones, A. E. and Kontak, D. J. (1998) Modeling fluid-rock interaction during greisenization at the East Kemptville tin deposit: implications for mineralization. Chem. Geol., 150, 1–17.

Hedenquist, J. W. and Lowenstern, J. B. (1994) The role of magmas in the formation of hydrothermal ore deposit. Nature, 370, 519–527.

Heinrich, C. A. (1990) The chemistry of hydrothermal tin(-tungsten) ore deposition. Econ. Geol., 85, 457–481.

Huang, G. F. (1992) Discussion on emplacement time of Qitianling composite rock masses. Geol. Prosp., 28, 7–11 (in Chinese with English abstract).

Huang, G. F., Zeng, Q. W., Wei, S. L., Xu, Y. M., Hou, M. S. and Kang, W. Q. (2001) Geological characteristics and ore-controlling factors of the Furong orefield, Qitianling, Hunan. Chinese Geol., 28, 30–34 (in Chinese with English abstract).

Huang, G. F., Gong, S. Q., Jiang, X. W., Tan, S. X., Li, C. B. and Liu, D. H. (2003) Exploration on the ore-forming regularities of tin deposits in Qitianling area, southern Hunan. Geol. Bull. China, 22, 445–451 (in Chinese with English abstract).

Jackson, K. J. and Helgeson, H. C. (1985) Chemical and thermodynamic constraints on the hydrothermal transport and deposition of tin: I. Calculation of the solubility of cassiterite at high pressures and temperatures. Geochim. Cosmochim. Acta, 49, 1–22.

Jiang, S. Y., Zhao, K. D., Jiang, Y. H., Ling, H. F. and Ni, P. (2006) New type of tin mineralization related to granite in south China: evidence from mineral chemistry, element and isotope geochemistry. Acta Petrol. Sin., 22, 2509–2516.

Keppler, H. and Wyllie, P. J. (1991) Partitioning of Cu, Sn, Mo, W, U and Th between melt and aqueous fluid in the systems haplogranite-H_2O-HCl and haplogranite-H_2O-HF. Contrib. Mineral. Petrol., 109, 139–150.

Lee, J. H. and Byrne, R. H. (1993) Complexation of trivalent rare earth elements (Ce, Eu, Gd, Tb, Yb) by carbonate ions. Geochim. Cosmochim. Acta, 57, 295–302.

Lehmann, B. (1990) Metallogeny of Tin. Springer Verlag, New York, 211p.

Lehmann, B. and Harmanto. (1990) Large-scale tin depletion in the Tanjungpandan tin granite, Belitung Island, Indonesia. Econ. Geol., 85, 99–111.

Li, R. Q. (1995a) Rare earth element distribution and its genetic signafication of calcite in Southern Hunan polymetallic metallogenic province. J. Mineral. Petrol., 15, 72–78 (in Chinese with English Abstract).

Li, R. Q. (1995b) Variation of Mg-Fe-Mn contents of calcite and its significance in Southern Hunan polymetallic Province. Hunan Geol., 14, 99–105 (in Chinese with English).

Li, H. L., Bi, X. W., Tu, G. C., Hu, R. Z., Peng, J., Shuang, Y., Li, Z. L., Li, X. M. and Yuan, S. D. (2007a) Mineral chemistry of biotite from the Qitianling granite associated with Furong tin deposit: tracing Sn-metallogeny signatures. Acta Petrol. Sin., 23, 2605–2614 (in Chinese with English abstract).

Li, Z. L., Hu, R. Z., Peng, J. T., Bi, X. W. and Li, X. M. (2006) Helium isotope geochemistry of ore-forming fluids from Furong tin orefield in Hunan Province, China. Resour. Geol., 56, 9–15.

Li, Z. L., Hu, R. Z., Yang, J. S., Peng, J. T., Li, X. M. and Bi, X. W. (2007b) He, Pb and S isotopic constraints on the relationship between the A-type Qitianling granite and the Furong tin deposit, Hunan Province, China. Lithos, 97, 161–73.

Li, T. Y. and Liu, J. Q. (2005) Characteristics and composition of fluid inclusions in Furong tin orefield, Qitianling area, South Hunan province. Geol. Mineral Resour. South China, 3, 44–49 (in Chinese with English abstract).

Linnen, R. L., Pichavant, M., Holtz, F. and Burgess, S. (1995) The effect of fO_2 on the solubility, diffusion, and speciation of tin in haplogranitic melt at 850°C and 2 kbar. Geochim. Cosmochim. Acta, 59, 1579–1588.

Linnen, R. L., Pichavant, M. and Holtz, F. (1996) The combined effects of fO_2 and melt composition on SnO_2 solubility and tin diffusivity in haplogranitic melts. Geochim. Cosmochim. Acta, 60, 4965–4976.

Loiselle, M. C. and Wones, D. R. (1979) Characteristics and origin of anorogenic granites. Geol. Soc. Am. Abstr. Prog., 11, 468.

London, D. (1987) Internal differentiation of rare-element pegmatites: effects of boron, phosphorus, and fluorine. Geochim. Cosmochim. Acta, 51, 403–420.

Lottermoser, B. G. (1992) Rare earth elements and hydrothermal ore formation processes. Ore Geol. Rev., 7, 25–41.

Lu, H. Z., Liu, Y. M., Wang, C. L., Xu, Y. Z. and Li, H. Q. (2003) Mineralization and Fluid Inclusion Study of the Shizhuyuan W-Sn-Bi-Mo-F Skarn Deposit, Hunan Province, China. Econ. Geol., 98, 955–974.

Mao, J. W., Wang, Z. L., Li, H. M., Wang, C. Y. and Chen, Y. C. (2003) Carbon and oxygen isotope components in the Permian basalt-hosted copper deposit in Ludian Area, Yunnan: implication for the mineralization process. Geol. Rev., 49, 610–615 (in Chinese with English abstract).

Mao, J. W., Li, X. F., Lehmann, B., Chen, W., Lan, X. M. and Wei, S. L. (2004) ^{40}Ar-^{39}Ar dating of tin ores and related granite in Furong Tin orefield, Hunan Province, and its geodynanmic significance. Mineral. Deposits, 23, 164–175 (in Chinese with English abstract).

Michard, A. (1989) Rare earth element systematics in hydrothermal fluids. Geochim. Cosmochim. Acta, 53, 745–750.

Michard, A., Albarede, F., Michard, G., Minster, J. F. and Charlou, J. L. (1983) Rare-earth elements and uranium in high-temperature solutions from East Pacific Rise hydrothermal ven field (13°N). Nature, 303, 795–797.

Mineyev, D. A. (1963) Geochemical differentiation of rare-earth elements. Geochem, 12, 1129–1149.

Möller, P. and Morteani, G. (1983) On the geochemical fractionation of ram earth elements during the formation of Ca-minerals and its application to problems of the genesis of ore deposits. In Augusthitis, S. S. (ed.) The significance of trace elements in solving petrogenetic problems and controversies. Theophrastus, Athens, 747–791.

Morgan, J. W. and Wandless, G. A. (1980) Rare earth element distribution in some hydrothermal minerals: evidence for crystallographic control. Geochim. Cosmochim. Acta, 44, 973–980.

Morishita, Y. (1993) Carbon and oxygen isotopic characteristics of epithermal veins in the Hokusatsu gold district, southern Kyushu, Japan. Resour. Geol., (14), 103–114.

Morishita, Y. and Nakano, T. (2008) Role of basement in epithermal deposits: the Kushikino and Hishikari gold deposits, southwestern Japan. Ore Geol. Rev., 34, 597–609.

Nilson, B. F. and Márcia, M. A. (1998) Granite-ore deposit relationships in Central Brazil. J. South Am. Earth. Sci., 11, 427–438.

O'Neil, J. R., Clayton, R. N. and Mayeda, T. K. (1969) Oxygen isotope fractionation in divalent metal carbonates. J. Chem. Phys., 51, 5547–5558.

Ohmoto, H. (1972) Systematics of sulfur and carbon isotopes in hydrothermal Ore deposits. Econ. Geol., 67, 551–578.

Ohmoto, H. and Rye, R. O. (1970) The Bluebell Mine, British Columbia; I, Mineralogy, paragenesis, fluid inclusions, and the isotopes of hydrogen, oxygen, and carbon. Econ. Geol., 65, 417–435.

Peng, J. T. and Hu, R. Z. (2001) Carbon and oxygen isotope systematics in the Xikuangshan giant antimony deposit, Central Hunan. Geol. Rev., 47, 34–41 (in Chinese with English abstract).

Peng, J., Zhou, M. F., Hu, R., Shen, N., Yuan, S., Bi, X., Du, A. and Qu, W. (2006) Precise molybdenite Re–Os and mica Ar–Ar dating of the Mesozoic Yaogangxian tungsten deposit, central Nanling district, South China. Mineral. Deposita, 41, 661–669.

Peng, J. T., Hu, R. Z., Bi, X. W., Dai, T. M., Li, Z. L., Li, X. M., Shuang, Y., Yuan, S. D. and Liu, S. R. (2007) $^{40}Ar/^{39}Ar$ isotopic dating of tin mineralization in Furong deposit of Hunan Province and its geological significance. Mineral. Deposits, 26, 237–248 (in Chinese with English abstract).

Pollard, P. J., Andrew, A. S. and Taylor, R. G. (1991) Fluid inclusion and stable isotope evidence for interaction between granites and magmatic hydrothermal fluids during formation of disseminated and pipe-style mineralization at the Zaaiplaats tin mine. Econ. Geol., 86, 121–141.

Qi, L., Hu, J. and Gregoire, D. C. (2000) Determination of trace elements in granites by inductively coupled plasma mass spectrometry. Talanta, 51, 507–513.

Rollinson, H. R. (1993) Using geochemical data: evaluation, presentation, interpretation. Longman Science and Technical & John Wiley and Sons, Inc., New York, 343p.

Rye, R. O., Hall, W. E. and Ohmoto, H. (1974) Carbon, hydrogen, oxygen, and sulfur isotope study of the Darwin Lead-Silver-Zinc deposit, Southern California. Econ. Geol., 69, 468–481.

Sawkins, F. J. (1984) Metal deposits in relation to plate tectonics. Springer-Verlag, Berlin, 315p.

Schade, J., Cornell, D. H. and Theart, H. F. J. (1989) Rare earth element and isotopic evidence for the genesis of the Prieska massive sulfide deposit, South Africa. Econ. Geol., 84, 49–63.

Schwartz, M. O. and Askury, A. K. (1989) Geologic, geochemical, and fluid inclusion studies of the tin granites from the Bujang Melaka Pluton, Kinta Valley, Malaysia. Econ. Geol., 84, 751–779.

Subías, I. and Fernandez-Nieto, C. (1995) Hydrothermal events in the Valle de Tena (Spanish Western Pyrenees) as evidenced by fluid inclusions and trace-element distribution from fluorite deposits. Chem. Geol., 124, 267–282.

Taylor, H. P. (1974) The application of oxygen and hydrogen isotope studies to problems of hydrothermal alteration and ore deposition. Econ. Geol., 69, 843–883.

Taylor, R. G. (1979) Geology of tin deposits. Elsevier Scientific Publishing Company, Amsterdam, 543p.

Taylor, J. R. and Wall, V. J. (1984) The mobilisation of tin from granitoid magmas, 27th Int. Geol. Congr, Moscow, p. 474.

Terakado, Y. and Masuda, A. (1988) The coprecipitation of rare-earth elements with calcite and aragonite. Chem. Geol., 69, 103–110.

Wang, D. H., Chen, Y. C., Li, H. Q., Chen, Z. H., Yu, J. J., Lu, Y. F. and Li, J. Y. (2003) Geological and geochemical features of the Furong tin deposit in Hunan and their significance for mineral prospecting. Geol. Bull. China, 22, 50–56 (in Chinese with English abstract).

Wang, X. W., Wang, X. D., Liu, J. Q. and Chang, H. L. (2004) Relationship of Qitianling granite to Sn mineralization in Hunan province. Geol. Sci. Technol. Inf., 23, 1–12 (in Chinese with English abstract).

Webster, J. D. and Holloway, J. R. (1990) Partitioning of F and Cl between magmatic hydrothermal fluids and highly evolved

granitic magmas. In Stein, H. J. and Hannah, J. L. (eds.) Ore-bearing Granite Systems: Petrogenesis and Mineralizing processes. Geological Society of America Special Paper, 246,21–34.

Wei, S. L., Zeng, Q. W., Xu, Y. M., Lan, X. M., Kang, W. Q. and Liao, X. Y. (2002) Characteristics and ore prospects of tin deposits in the Qitianling area, Hunan. Geol. China, 29, 67–75 (in Chinese with English abstract).

Wood, S. A. (1990) The aqueous geochemistry of the rare-earth elements and yttrium: 1. Review of available low-temperature data for inorganic complexes and the inorganic REE speciation of natural waters. Chem. Geol., 82, 159–186.

Xu, Y. M., Hou, M. S., Liao, X. Y. and Ao, Z. W. (2000) Deposit types and prospect for prospecting of Sn deposits in Furong ore field, Chenzhou. Hunan Geol., 19, 95–100 (in Chinese with English abstract).

Yuan, S. D., Peng, J. T., Shen, N. P., Hu, R. Z. and Dai, T. M. (2007) ^{40}Ar-^{39}Ar isotopic dating of the Xianghualing Sn-polymetallic orefield in Southern Hunan, China and its geological implications. Acta Geol. Sin. (English Ed.), 81, 278–286.

Zhang, L. G. (1985) The application of Stable isotopes in geological sciences. Shanxi Scientific Publication, Xi'an, 267p.

Zhao, K. D., Jiang, S. Y., Jiang, Y. H. and Wang, R. C. (2005) Mineral chemistry of the Qitianling granitoid and the Furong tin ore deposit in Hunan Province, South China: implication for the genesis of granite and related tin mineralization. Eur. J. Mineral., 17, 635–648.

Zheng, Y. F. (1990) Carbon-oxygen isotopic covariation in hydrothermal calcite during degassing of CO_2. Mineral. Deposita, 25, 246–250.

Zheng, Y. F. and Hoefs, J. (1993) Carbon and oxygen isotopic covariations in hydrothermal calcites. Mineral. Deposita, 28, 79–89.

Zheng, Y. F. and Chen, J. F. (2000) Stable isotope geochemistry. Scientific Publishing House, Beijing, 316p (in Chinese).

Zheng, J. J. and Jia, B. H. (2001) Geological characteristics and related tin-polymetallic mineralization of the Qitianling granite complex in Southern Hunan Province. Geol. Mineral. Resour. South China, 4, 50–57 (in Chinese with English abstract).

Zhong, S. and Mucci, A. (1995) Partitioning of rare earth elements (REEs) between calcite and seawater solutions at 25°C and 1 atm, and high dissolved REE concentrations. Geochim. Cosmochim. Acta, 59, 443–453.

Zhu, J. C., Huang, G. F., Zhang, P. H., Li, F. C. and Rao, B. (2003) On the emplacement age and material sources for the granites of Cailing Superunit, Qitianling pluton, South Hunan Province. Geol. Rev., 49, 245–252 (in Chinese with English abstract).

Zhu, J. C., Zhang, H., Xie, C. F., Zhang, P. H. and Yang, C. (2005) Zircon SHRIMP U-Pb geochronology, petrology and geochemistry of the Zhujianshui Granite, Qitianling pluton, Southern Hunan Province. Geol. J. China Univ., 11, 335–342 (in Chinese with English abstract).